Study by Molecular Docking of the interactions between dihydroorotate dehydrogenase and a series of inhibitors of pyrrole derivatives for the treatment of malaria

Abstract

Malaria, although a curable disease, continues to be the most important infectious disease in terms of incidence and mortality worldwide. It is a potentially fatal disease caused by parasites transmitted to people through the bites of infected female Anopheles mosquitoes. This disease affects more than 216 million people and kills a million, mainly children and pregnant women.Anti-malaria therapy finds itself confronted with drug-resistant strains, hence the urgency of finding new targets and new anti-infectious agents. Dihydroorotate dehydrogenase (DHODH) is an essential enzyme for the design of new antimalarial drugs.Using a Computer Aided Molecular Design (CAMD) reaction approach, a series of 17 molecules from the pyrrole family, inhibitors of (DHODH) was designed within the protein (PDB code: 6VTN). These molecules with known IC_{50} were selected to build an RQSAR model presenting a linear correlation between the Gibbs energy (ΔΔG), the complexes formed and the experimental inhibition potential(pIC_{50}^{exp}) : pIC_{50}^{exp}= - 0.2909×ΔΔG+ 7.7715 ; R^2 = 0,97.we subsequently carried out a studyon the catalyticresidues(interaction by residue) in order to exploit the different interactions (enzyme: inhibitor).The predictive power of the QSAR model was validated by the generation of 3D-QSAR pharmacophores (PH4): $pIC_{50}^{exp} = 0.9939 \times pIC_{50}^{est} + 0.0421$; R^2 = 0.92.

Keywords: QSAR model; pharmacophore model; molecular docking; molecular modeling; Dihydroorotate dehydrogenase; pyrrole family.

1. INTRODUCTION

Despite the efforts and resources devoted to the fight against malaria, also the knowledge acquired on the various species of plasmodium, of which plasmodium faciparum is the most common in humans[1],malaria remains the world's leading parasitic endemic. According to the World Health Organization (WHO), the number of cases due to malaria in 2022 globally is 249 million and the number of deaths linked to this disease has been estimated at 608,000.However, the African region bears a large and disproportionate share of the global malaria burden. In 2023, 94% of malaria cases (246 million) and 95% of deaths from the disease (569,000) were recorded on the African continent according to the World Health Organization (WHO). One of the factors which has contributed to the deterioration of the malaria situation in recent years is the appearance of multiple resistances of parasites to different antimalarial molecules and the progressive extension of mosquito resistance to insecticides[2, 3].Thus, the race towards the development of new control tools, and new, more active, inexpensive drugs becomes an imperative. It is in this context that several approaches have been developed, including Computer-Aided Design of Tailored Molecules (CADTM), which has become a powerful tool for discovering new drugs.The objective of this work is to carry out a structural analysis of the interactions taking place between the malaria parasitic protease dihydroorotate dehydrogenase and inhibitors derived from molecules derived from pyrroles in order to develop antimalarial molecules. Thus, the stability of the three-dimensional structure of a molecule is determined by intramolecular interactions and interactions with the external environment. The search for stable conformations of a molecule therefore consists of determining the minima of the overall interaction energy[4].We will proceed by developing a Quantitative Structure Activity Relationship (QSAR) “Protein: Inhibitor” (P: I) model, to describe intermolecular interactions. This development of the QSAR model will be carried out initially by a study of the interactions between dihydroorotate dehydrogenase and molecules derived from pyrroles by molecular docking then followed by an in-depth study of interaction by residues, and finally we will end with a study based on molecular structures using the 3D pharmacophore method.

2. MATERIALS AND METHODS

2.1. Receiver (Dihydroorotate Dehydrogenase)

Dihydroorotate dehydrogenase is a mitochondrial enzyme providing an excellent model to study the evolutionary divergence of catalytic and structural features of proteins [5]. The active site (figure 1) of dihydroorotate dehydrogenase around a radius of 10 Å isolated in Plasmodium falciparum provides very interesting information for the discovery of new powerful inhibitors for the treatment of malaria [6]. However, this binding site is located in a highly hydrophobic region [7]. Furthermore, this binding site is surrounded mainly by hydrophobic amino acid side chains, thus favoring hydrophobic interactions with non-polar groups (Figure 7) [8].

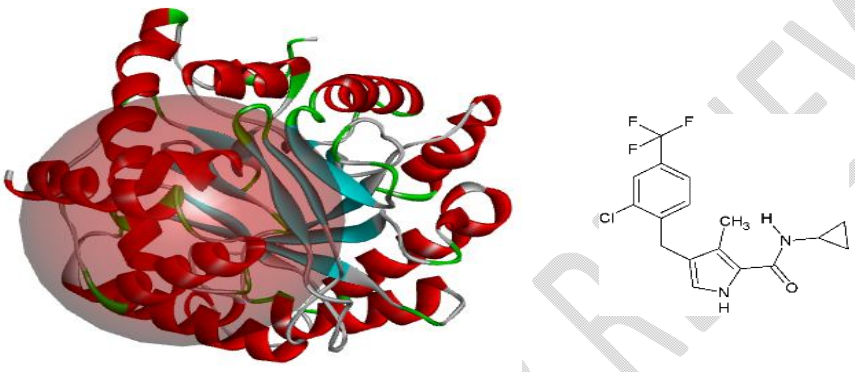

Figure 1.On the left crystallographic structure of DHODH (PDB code: 6VTN) with within it a red colored sphere illustrating the active site, on the right the endogenous ligand (Pyl 1).

2.2. Ligands (pyrroles Derivatives)

Pyrrole derivatives have been the recent target of numerous methodologies due to their pharmacological action in the context of DHODH inhibition [9]. The inhibitors that we used throughout this work come from the literature [9]. Indeed, the study of the structure-activity ratio (SAR) of this new series of molecules derived from pyrrole was carried out in order to obtain new agents which could be optimized as effective molecules in the fight against malaria [10]. Out of a total of 17 inhibitors, 14 (Pyl 1 to Pyl 14) were chosen for the Training set and 3 (Pyl 15 to Pyl 17) for the validation set (Table 1). Their inhibition constant is between 0.01 µM and 10 µM (Table 1).

Table 1. Training sets (Pyl 1 to Pyl 14) and validation set (Pyl 15 to Pyl 17) of dihydroorotate dehydrogenase inhibitors used in the preparation of QSAR models.

Training set	Pyl 1	Pyl 2	Pyl 3	Pyl 4	Pyl 5	Pyl 6	Pyl 7	Pyl 8	Pyl 9	Pyl 10	Pyl 11
IC_{50} (µM)	0.01	0.02	0.03	0.04	0.04	0.04	0.07	0.08	0.17	0.21	0.45

Training set	Pyl 12	Pyl 13	Pyl 14
IC_{50} (µM)	1.1	2.5	10

Validation set	Pyl 15	Pyl 16	Pyl 17
IC_{50} (µM)	0.18	0.12	0.88

These inhibitors derived from pyrrole derivatives are of the micro molar order and are presented in Figure 2.

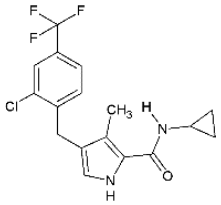

Pyl 1

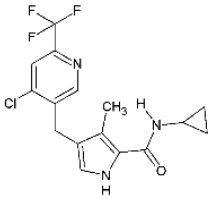

Pyl 2

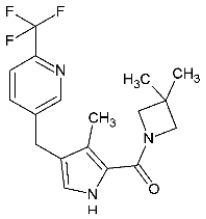

Pyl 3

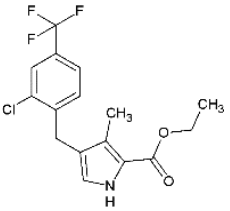

Pyl 4

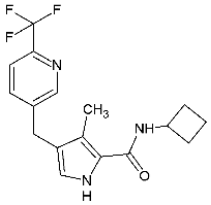

Pyl 5

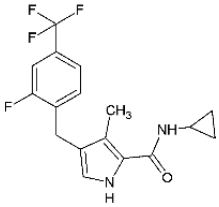

Pyl 6

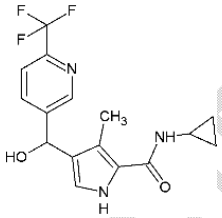

Pyl 7

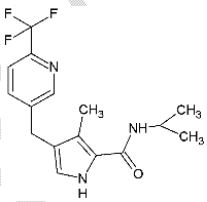

Pyl 8

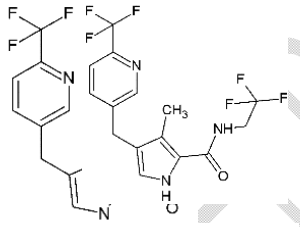

Pyl 10

Pyl 11

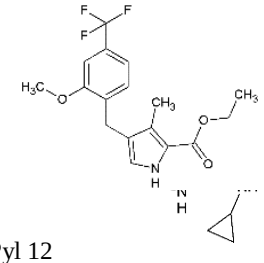

Pyl 12

Pyl 9

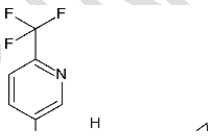

Pyl 13

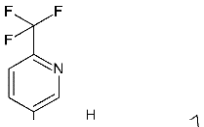

Pyl 14

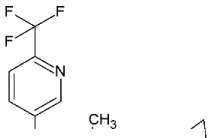

Pyl 15

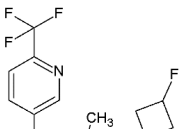

Pyl 16

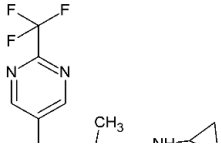

Pyl 17

Figure 2. Inhibitors ofdihydroorotate dehydrogenase

2.3. Molecular Docking

Interactions between proteins are the basis of most biological mechanisms [11]. The details of these interactions, at the molecular level, are therefore of great interest for the development of drugs [12]. A fundamental step in the molecular docking strategy is the identification of amino acid residues that can be involved in the ligand recognition process.Binding energy is the energy of binding a ligand (L) to a receptor (R). Its value in this work is approximated to that of the free enthalpy of formation of the enzyme-inhibitor complex. These binding energies ($\Delta Gbinding$) were calculated for each complex after their minimization using the "Calculate Binding Energy" protocol. Chemical equilibrium of ligand-receptor interaction.

$$\boldsymbol{L + R \rightleftharpoons C} \quad (1)$$

$$\boldsymbol{\Delta G_{complex} = G_{complex} - G_{ligand} - G_{receptor}} \quad (2)$$

$$\boldsymbol{\Delta\Delta G_{(receptor+ligand)} = \Delta G_{(receptor+ligand)} - \Delta G_{(receptor+endogenous\ ligand)}} \quad (3)$$

$$\boldsymbol{\Delta\Delta G_{binding} = \Delta G_{binding} - \Delta G_{binding\ ref}} \quad (4)$$

$\Delta G_{\text{binding ref}}$is the binding energy of the most active ligand.

As the$\mathbf{IC_{50}^{exp}}$of the various inhibitors are known from the literaturethe $\mathbf{pIC_{50}^{exp}}$calculated using the following formula:

$$\boldsymbol{pIC_{50}^{exp} = -\log_{10}\left(IC_{50}/10^{6}\right)} \quad (5)$$

2.4.Interaction Energy by Residue

The calculation of the interaction energy Eint between the enzyme (E) and the inhibitor(I)is done using a protocol available in Discovery Studio [13]. It makes it possible to calculate the non-bonding interactions (van der Waals and electrostatic terms) between the enzyme and the ligand. Calculations are performed by applying the CFF force field with a dielectric constant equal to 4[14].The decomposition of the interaction energy into individual contributions from each active site residue is an indicator of affinity between the enzyme and the 'inhibitor. Indeed, the diagrams constructed from the individual contributions of each residue of the active site make it possible to compare them at the level of the three categories of inhibitors which are the most active inhibitors, the moderately active and the least active. The results from these comparisons can justify the contribution of catalytic residues and certain active site residues to the variation in biological activity.

2.5. Pharmacophore Model

The interaction generation protocol of the Discovery Studio molecular modeling program [13] provides the pharmacophore functionalities of the protein active site. The dihydroorotate dehydrogenase protein presents a hydrophobic pocket within its active site (Figure 1). The 3D-RQSA pharmacophore for dihydroorotate dehydrogenase inhibition was generated from the active conformations of the 14 ligands from the training set (Pyl 1 to Pyl 14) and evaluated by the other 3 from the validation set (Pyl 15 to Pyl 17) covering a wide range of activities experimental (0.01 - 10 µM). The generation process takes place in three main stages: the constructive stage, the subtractive stage and the optimization stage [15] described by the work of Niaré et *al*. At the end of the optimization, the 10 best performing pharmacophore hypotheses were kept [15]. The pharmacophore model constructed from the 14Pyl of the test set was then evaluated by the 3 Pyl inhibitors of the validation set [15]. By applying the "Ligand Pharmacophore Mapping" protocol which uses HypoGen from DS Catalyst [13], we map these 3 inhibitors based on the functionalities of the PH4 constructed. Thus, we evaluate their forecast activities

IC_{50} and using equation 6 we deduce their$\mathrm{pIC}_{50}^{\mathrm{pred}}$.The ratio$pIC_{50}^{exp}$/ pIC_{50}^{pred} of each of the 3 inhibitors is calculated and compared to 1.

3. RESULTS AND DISCUSSION

3.1. Molecular Docking

We carried out the molecular docking of 17 pyrrole-derived inhibitors within the active site of dihydroorotate dehydrogenase. The analysis of the binding mode between the ligand and the protein allowed us to select the best poses among the numerous conformations generated by the docking algorithm. We calculated the binding energies ($\Delta\mathbf{G}_{\mathbf{binding}}$). These results are presented in Table 2 below.The correlation curve between the variation in binding energies and the experimental $\mathrm{pIC}_{50}^{\mathrm{exp}}$ of the 14 inhibitors in the test set is shown in Figure. 3

Table 2. Protein-ligand binding energy and biological activities

Nature	LIGANDS	$\Delta\mathbf{G}_{\mathbf{binding}}$ (kcal/mol)	$\Delta\Delta\mathbf{G}_{\mathbf{binding}}$ (kcal/mol)	$\mathbf{IC}_{\mathbf{50}}^{\mathbf{exp}}$ (μM)	$\mathbf{pIC}_{\mathbf{50}}^{\mathbf{exp}}$
Molecules more active	Pyl 1	-51.09	0	7.76	0.01
	Pyl 2	-50.9	0.19	7.69	0.02
	Pyl 3	-50.8	0.29	7.48	0.03
	Pyl 4	-50.08	1.01	7.37	0.04
Medium-active molecules	Pyl 5	-49.93	1.16	7.35	0.04
	Pyl 6	-49.83	1.26	7.35	0.04
	Pyl 7	-48.71	2.38	7.13	0.07
	Pyl 8	-47.69	3.40	7.09	0.08
	Pyl 9	-47.01	4.08	6.76	0.17
Molecules Weakly active	Pyl 10	-46.86	4.23	6.67	0.21
	Pyl 11	-45.7	5.39	6.34	0.45
	Pyl 12	-45.26	5.83	5.95	1.1
	Pyl 13	-43.81	7.28	5.60	2.5
	Pyl 14	-42.34	8.75	5	10

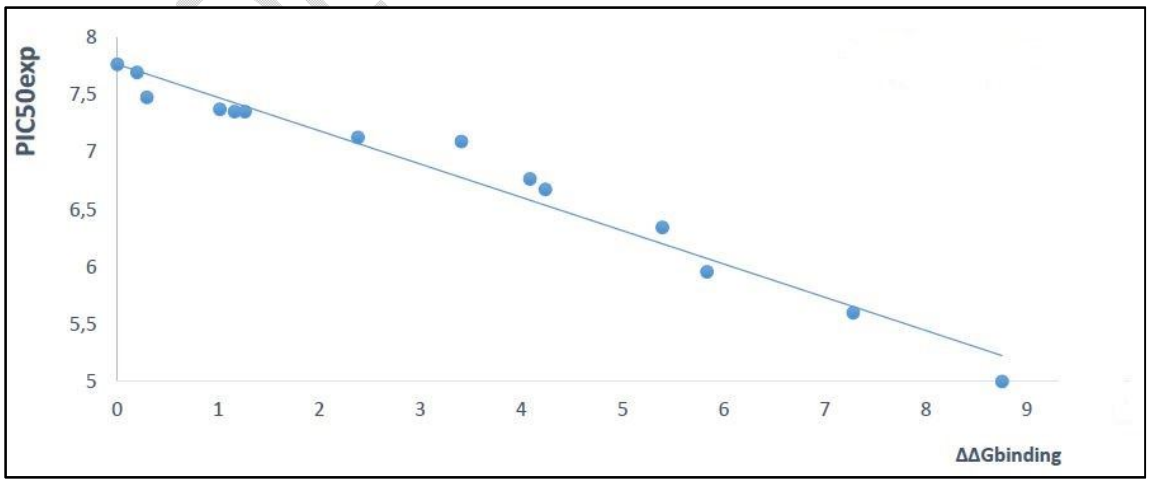

Figure 3. Plot illustrating the correlation between $\mathbf{pIC}_{\mathbf{50}}^{\mathbf{exp}}$and the $\Delta\Delta\mathbf{G}_{\mathbf{binding}}$ energy component.

Table 3. Statistical data and linear regression

Number of compounds n	14
Correlation coefficient of the regression line R^2	0.97
Cross-validation coefficients R^2_{CV}	0.96
Standard error of the regression(σ)	0.071
Fisher test (F)	341.39
Confidence level	95%
Risk of error	5%
Experimental biological activity range (μM)	0.01 – 10

Table 4. Comparison of experimental and theoretical biological activity values in the validation set

Ligands	$\Delta G_{binding}$ **(kcal/mol)**	$\Delta\Delta G_{binding}$ **(kcal/mol)**	IC_{50}^{exp} (μM)	IC_{50}^{exp}	pIC_{50}^{pre}	$pIC_{50}^{Pre} / pIC_{50}^{exp}$
Pyl 15	-49.61	1.48	0.18	7.74	7.34	0.95
Pyl 16	-47.90	3.19	0.12	6.92	6.84	0.99
Pyl 17	-45.76	5.33	0.88	6.22	6.22	1.02

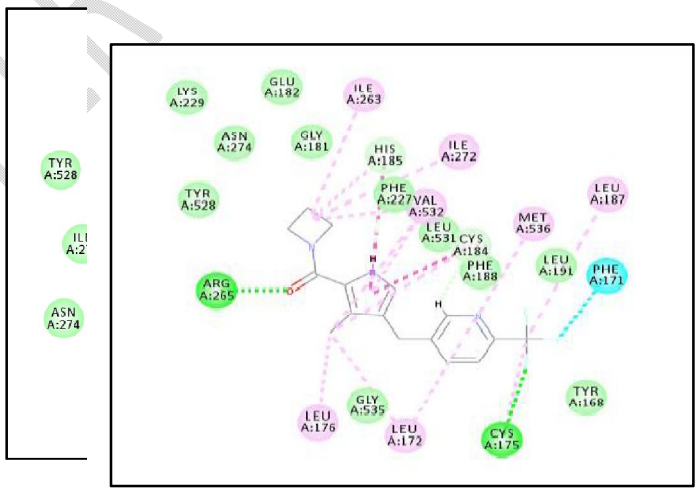

Figure 4.2D diagram of the active ligand Pyl 1

Figure 5. 2D diagram of the moderately active ligand Pyl 9

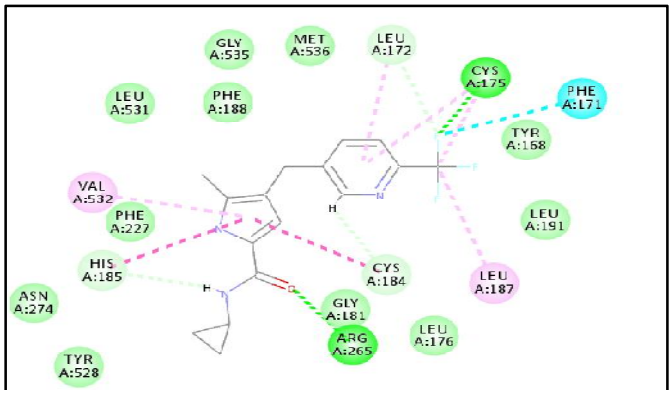

Figure 6. 2D diagram of the less active ligandPyl 14

The correlation line (Figure 3) with equation $\boldsymbol{pIC_{50}^{exp} = -0.2909 \times \Delta\Delta G_{binding} + 7.7715}$predicts the activitypredicted DHODH inhibitors. For the molecules in the validation set, the predicted activities will be compared to the experimental activities in order to judge this prediction. The prediction is good if the ratio $\boldsymbol{pIC_{50}^{théo}/pIC_{50}^{préd}}$ is close to 1. The predicted biological activities of the ligands in the validation set are calculated from the following equation:

$$\boldsymbol{pIC_{50}^{pred} = -0.2909 \times \Delta\Delta G_{binding} + 7.7715} \quad (6)$$

Then, these predicted values are compared to the experimental values. Table 4 presents these relationships. These ratios are close to 1. This confirms that the model is reliable and that from it the activities of new analogues can be estimated.The residues present within the active site of DHODH in a 10 Å environment are as follows:Phe 171, Cys 175, Val 532, His 185, Arg 265, Leu 176, Cys 184, Gly 535, Leu 172, Met 536, Tyr 168, Leu 187. The three classes of inhibitors, notably the most active inhibitors, the moderately active and the medium active, interact with these different residues listed above in order to obtain the most probable optimization.These interactions are of different nature and are as follows: a hydrogen interaction, a π- π-T Shaped interaction, an amide- π Stacked interaction, an Alkyl interaction and a π- Alkyl interaction. The most active ligand (Pyl 1) establishes a hydrogen interaction with Arg 265 and another with Cys 175; a π-π-T Shaped interaction with Cys184 and another with His 185; an amide-π Stacked interaction with Val 532; an Alkyl interaction with Leu 176, Val 532; Cys 184; Leu 172, Leu 187; Cys 175 and Met 536 and finally a π-Alkyl interaction with Met 536 (Figure 4).Le ligand moyennement actif **(**Pyl9) établit une interaction hydrogène avec Arg 265 et une autre interaction avec Cys 175 ; une interaction π- π-T Shaped avec His185 et une autre avec Cys 184 ; une interaction amide-π Stackedavec Val 532 ; une interaction Alkyl avec Ile 263, Ile 272, Val 532, Leu 176, Leu 172 et une autre interaction π- Alkyl avec Val 532 (Figure 5).As for the least active ligand (Pyl 14), it establishes a hydrogen interaction with Arg 265 and another interaction with Cys 175; a π-π-T Shaped interaction with His 185 and another Cys 184 interaction; an amide-π interaction Stacked Val 532; an Alkyl interaction with Cys 175 and Leu 187 and finally another π- Alkyl Leu172 and Cys 175 interaction (Figure 6).After analyzing the different interactions, the observation made is that the presence of Alkyl interactions are observed in all the complexes, but 8 for the most active complex, 5 for the moderately active complex and 2 for the weakly active complex. Indeed, these Alkyl interactions are hydrophobic in nature and contribute to the rigidity of the complexes. In addition, the ligand (Pyl 1) occupies more hydrophobic pockets than the other ligands. Which therefore makes it more active. For π-π-T Shaped interactions, they are present in all the complex at number 2 per complex. Regarding Stacked π-amides, they are present in all the complex with the same residue. The number of Alkyl interactions decreases for moderately and weakly active ligands compared to the active ligand. Hydrogen interactions contributing to the stability of complexes are present in all complexes.

3.2. Energy by residue

The energetic understanding of the different ligands (Pyl x) used in DHODH inhibition is also provided by the energetic interaction diagram (IE; ΔEint). The distribution of the interaction energy in contribution of the residues to the active site of DHODH is in three classes: a first class of ligands with maximum biological activity (Figure 7), a second class of ligands with moderate biological activity (Figure 8) and a third class of ligands with the lowest biological activities (Figure 9).

Table 5. Values of energy contributions expressed in kcal.mol-1 of active site residues interacting with the most active ligands (Pyl1 to Pyl4).

	most active ligands			
	Pyl 1	Pyl 2	Pyl 3	Pyl 4
Tyr 168	-3.36	-3. 43	-3 .89	-3. 38
Phe 171	-1.89	-1. 89	-1.71	-1.91
Leu 172	-0.18	-0.32	-0.45	-0.12
Cys 175	-0.83	-0.74	-0.77	-0.88
Leu 176	-1.59	-1.55	-1.26	-1.40
Cys 184	-4.10	-4.73	-4.88	-3.24
His 185	-5.54	-5.52	-5.06	-5.43
Leu 187	-1.95	-1.89	-1.95	-1.96
Arg 265	-5.65	-5.71	-5.39	-5.67
Tyr 528	-1.47	-1.50	-1.34	-1.10
Val 532	-6.26	-6.37	-6.17	-6.00
Gly 535	-1.08	-1.95	-1.75	-1.09
Met 536	-0.43	-0.39	-0.17	-0.49

Table 6. Values of energy contributions expressed in kcal.mol-1 of active site residues interacting with the Medium-active ligands (Pyl 5 to Pyl 9).

	Medium-active ligands				
	Pyl 5	Pyl6	Pyl7	Pyl8	Pyl9
Tyr 168	-2.81	-2.97	-2.84	-2.82	-2.81
Phe 171	-1.71	-1.85	-1.87	-1.71	-1.92
Leu 172	-4.44	-4.17	-4.07	-4.49	-4.88
Cys 175	-0.76	-0.87	-0.82	-0.77	-0.77
Leu 176	-1.24	-1.56	-1.53	-1.22	-1.23
Cys 184	-4.86	-4.10	-4.09	-4.95	-4.86
His 185	-5.07	-5.54	-5.62	-5.99	-5.08
Leu 187	-1.94	-1.93	-1.94	-1.94	-1.99
Arg 265	-5.07	-5.63	-5.53	-5.10	-5.06
Tyr 528	-1.79	-1.47	-1.43	-1.03	-1.79
Val 532	-6.16	-6.09	-6.25	-6.48	-6.19
Gly 535	-1.47	-1.33	-1.96	-1.47	-1.55
Met 536	-2.83	-2.07	-2.83	-2.82	-2.82

Table 7. Values of energy contributions expressed in kcal.mol-1 of active site residues interacting with the Weakly active ligands (Pyl10 to Pyl14).

	Weakly active ligands				
	Pyl10	Pyl11	Pyl12	Pyl13	Pyl14
Tyr 168	-2.84	-2.89	-2.32	-2.85	-2.86
Phe 171	-1.74	-1.89	-1.95	-1.93	-1.9
Leu 172	-4.48	-4.36	-4.31	-4.00	-4.02
Cys 175	-1.97	-1.11	-1.90	-1.77	-1.75
Leu 176	-1.24	-1.15	-1.60	-1.83	-1.94
Cys 184	-4.65	-4.92	-4.61	-4.52	-4.55
His 185	-5.72	-5.48	-5.61	-5.43	-5.82
Leu 187	-1.94	-1.95	-1.99	-1.90	-1.93
Arg 265	-5.29	-5.29	-5.11	-5.33	-5.26
Tyr 528	-1.06	-1.50	-1.13	-1.14	-1.52
Val 532	-5.19	-5.34	-5.14	-5.30	-5.41
Gly 535	-0.45	-0.72	-0.99	-0.49	-0.51
Met 536	-3.80	-3.93	-3.37	-3.07	-3.24

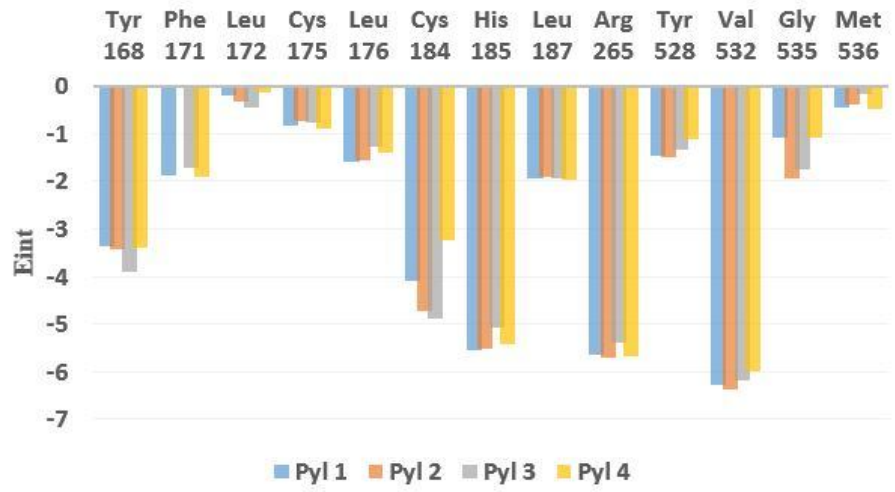

Figure 7. Individual contributions of interaction energies of active site residues with the most active ligands (Pyl 1 to Pyl 4) expressed in kcal.mol-1.

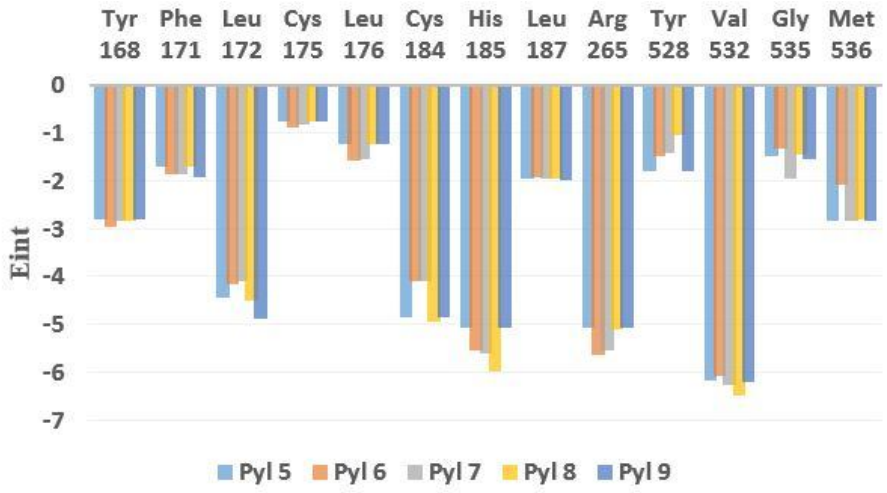

Figure 8. Individual contributions of interaction energies of active site residues with the Medium-active ligands(Pyl5 to Pyl9) expressed in kcal.mol-1.

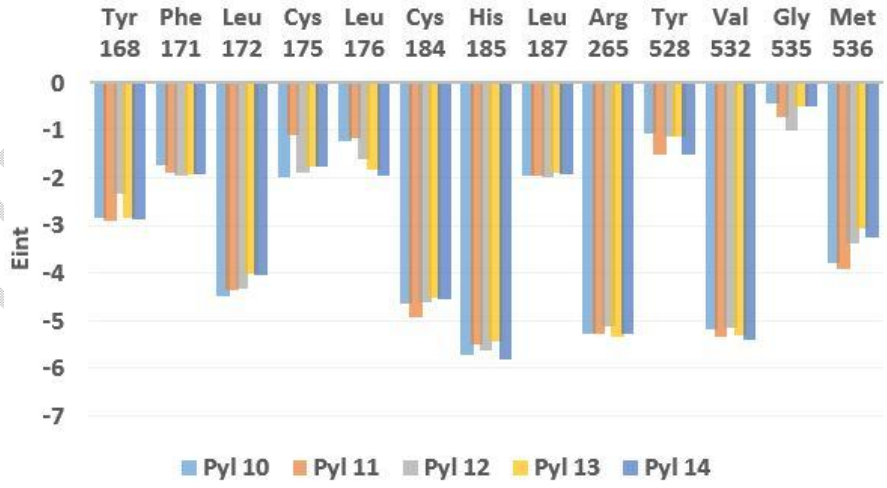

Figure 9. Individual contributions of interaction energies of active site residues with the Medium-active ligands (Pyl 5 to Pyl 9) expressed in kcal.mol-1.

For all classes, the interaction energy per residue is strongest with residues Val 532, Arg 265, His 185 and Cys 184 and it is moderate with residues Tyr 168, Phe 171, Leu 187 and Leu 176. is interesting to analyze within class 1 to class 3, the difference in energy contribution of the catalytic residue Val 532 which establishes an amide-π Stacked interaction with the pyrrole ring of each inhibitor. This energy contribution at the level of Pyl1 (IC_{50}^{exp}= 7.76 µM) is -6.26 kcal.mol^{-1}, at the level of Pyl 9 (IC_{50}^{exp} = 7.69 µM) it is -6.16 kcal .mol^{-1} as to the level of Pyl 14 (IC_{50}^{exp}= 5.00 µM) it is -5.19 kcal.mol^{-1}. Indeed, this major energy difference largely contributes to the inhibition of DHODH.

3.3. Pharmacophore Model

After running the "3D QSAR Pharmacophore Generation" protocol with DS, 10 hypotheses were generated. The characters of these hypotheses are given in Table 8. After visualization to analyze the superposition of the common parts of the test set ligands, hypothesis 1 having the smallest value of the RMSD (best RMSD) and the largest value of R ^{2} (best R ^{2}) was chosen. Based on this hypothesis, the values of the activities IC_{50}^{est} could be noted and the PIC_{50}^{est} of the 14 poses retained from the test set were calculated and assigned in table 9. The line of regression of this pharmacophore is illustrated through Figure 10. In addition, an analysis of the statistical data of this regression line is made and the results are recorded in the table 10. This model was validated by calculating the theoretical activities of the molecules in the validation set from the equation:

$$\boldsymbol{pIC_{50}^{exp} = 0.9939 \times +0.0421 pIC_{50}^{est}} \qquad (7)$$

Table 8. Different pharmacophore hypotheses and their characteristics

Hypothesis	RMSD	R^2	Total cost
Hypothesis 1	1.17782	0.959917	52.7442
Hypothesis 2	1.18484	0.959437	52.9166
Hypothesis 3	1.18484	0.959437	52.9166
Hypothesis 4	1.22375	0.956665	53.5608
Hypothesis 5	1.22375	0.956665	53.5608
Hypothesis 6	1.26185	0.953866	54.2764
Hypothesis 7	1.27674	0.952733	54.4794
Hypothesis 8	1.2822	0.952318	54.582
Hypothesis 9	2.13326	0.861722	76.0681
Hypothesis 10	2.33545	0.831401	81.6311
FixedCost	0	0	42 .9788
NullHypothesis	4.20174	0	157.807

Table 9. Experimental activity values and those predicted by the pharmacophore model

Ligands	$IC_{50}^{est}(\mu M)$	pIC_{50}^{est}	$IC_{50}^{exp}(\mu M)$	pIC_{50}^{exp}
Pyl 1	0.02	7.63	0.01	7.77
Pyl 2	0.01	7.74	0.02	7.69
Pyl 3	0.03	7.48	0.03	7.48

Pyl 4	0.04	7.39	0.04	7.37
Pyl 5	0.11	6.95	0.04	7.36
Pyl 6	0.03	7.46	0.04	7.35
Pyl 7	0.09	7.04	0.07	7.13
Pyl 8	0,10	7.00	0.08	7.09
Pyl 9	0.02	7.63	0.01	7.76
Pyl 10	0.02	7.74	0.02	7.70
Pyl 11	0.03	7.48	0.03	7.48
Pyl 12	0.04	7.39	0.04	7.37
Pyl 13	0.11	6.95	0.04	7.36
Pyl 14	0.03	7.46	0.04	7.35

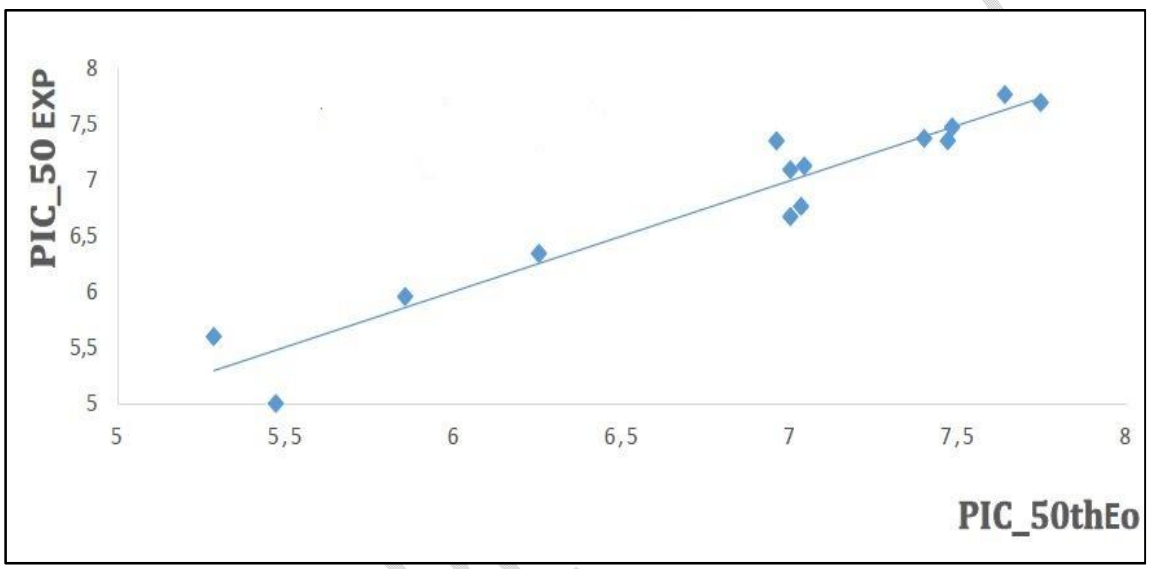

Figure 10. Correlation graph of experimental inhibitory activity versus predicted inhibitory activity

Table 10. Statistical data and linear regression

Number of compounds n	14
Correlation coefficient of the regression line R^2	0.92
Cross-validation coefficients R^2_{CV}	0.91
Standard error of the regression(σ)	0.58
Fisher test (F)	137.04
Confidence level	95%
Risk of error	5%
Experimental biological activity range (μM)	0.01 – 10

Table 11. Comparison between pIC_{50}^{est} and pIC_{50}^{exp} of the ligands in the validation set

LIGANDS	IC_{50}^{est}	pIC_{50}^{est}	pIC_{50}^{exp}	Ratios
Pyl 15	0.18	7.74	7.75	1.00
Pyl 16	0.12	6.92	6.92	1.00
Pyl 17	0.88	6.06	6.05	0.99

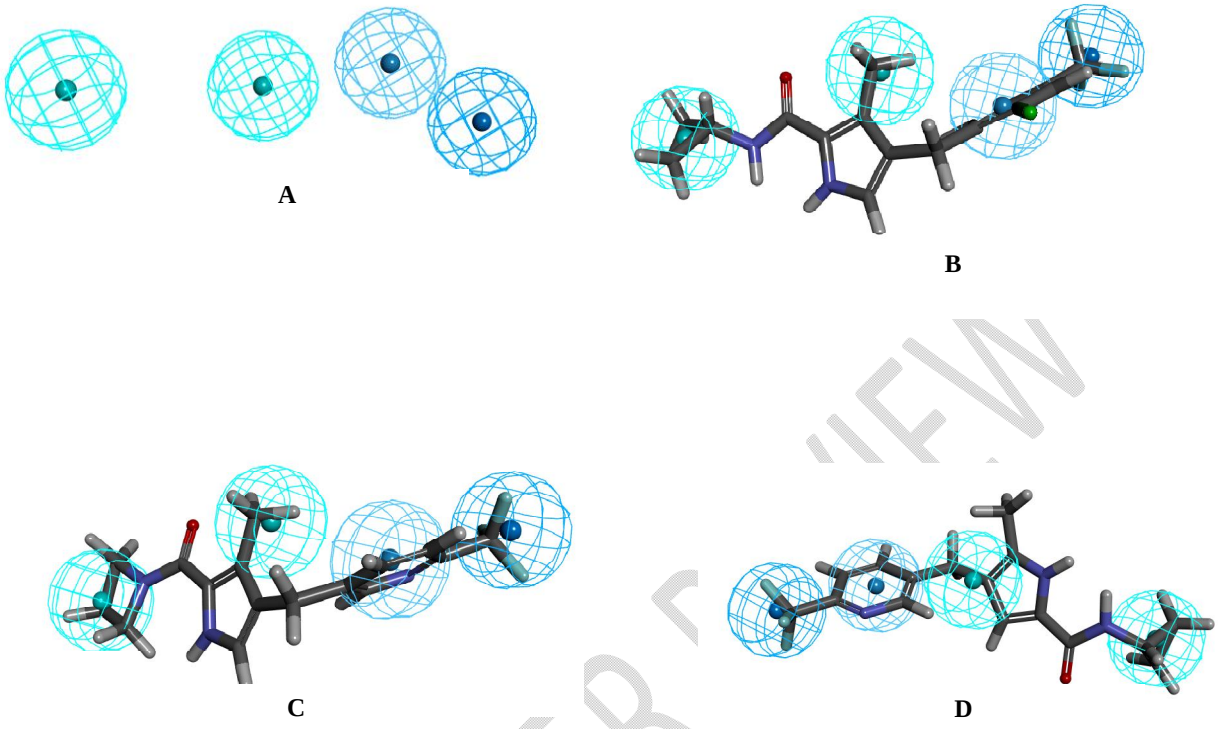

Figure 11. (A) Features coordinates of centers,(B) mapping of pharmacophore of DHODH inhibitor with the most potent molecule Pyl1, (C) mapping of pharmacophore of DHODH inhibitor with Medium-activemoleculePyl 9, (D) mapping of pharmacophore of DHODH inhibitor with Weakly active molecule Pyl 14. Feature legend: HYDA = Hydrophobic Aliphatic (blue), HYD = Hydrophobic(cyan).

For a good PH4 model, "Fixedcost" must be lower than "Null Hypothesis" and the difference (Δ) between these two identities (Fixedcost and Null Hypothesis) must be greater than 70. According to our results from Table 8, Fixedcost is equal to 42.98 and Null Hypothesis is equal to 157.81 which shows that Fixedcost is lower than Null Hypothesis, moreover, the difference(Δ = 157.81 - 42 .98 = 114.83)is greater than 70 representatives thus the quality of the PH4 model. The ratio (PIC_{50}^{est}/ PIC_{50}^{exp}) estimated activities (PIC_{50}^{est}) and experimental(PIC_{50}^{exp})taken from Table 11 is close to 1, which perfectly confirms the predictive quality of the PH4 model used. The PH4 model selected highlights 04 hydrophobic features including 2 Hydrophobic (HYD) features in cyan color and 2 Hydrophobic Aliphatic (HYDA) features in blue color. The active ligand (Pyl 1) aligns perfectly with the pharmacophore model (Figure 10). The cyan colored spheres occupy the Methyl and cyclopropyl groups which are aliphatic hydrophobic groups. The spheres in blue occupy an aromatic ring which is an aromatic hydrophobic group and also a substituted Methyl group. This perfect superposition justifies the strong biological activity of this ligand. The moderately active ligand (Pyl 9) matches all the features perfectly except one: the blue sphere of the aliphatic hydrophobic group. In terms of activity, it is less active than the first ligand (Pyl 1). As for the weakly active ligand (Pyl 14), it only matches three features of our model. However, the cyan colored sphere does not align perfectly with the aliphatic hydrophobic group which is the Methyl group; on the contrary it moves away from this grouping of the Methyl group. This poor alignment clearly justifies the ineffectiveness of this ligand (Figure 10).

4. CONCLUSION

This present work is part of a study of interaction between the malaria parasite protein dihydroorotate dehydrogenase (DHODH) and a series of 17 inhibitors, all derived from the pyrrole molecule (Pyl). Carrying out this work required knowledge of computer simulation, particularly molecular modeling techniques and computer-assisted combinatorial chemistry. These techniques prove to be more than necessary in the development of new drugs intended to fight against certain endemic diseases such as malaria. The objective of this work is of paramount importance due to the alarming statistics from the World Health Organization (WHO).Faced with this urgent need, the discovery and development of new therapeutic targets and new molecules are therefore required in order to expand the antimalarial arsenal. The different methods used, namely molecular docking, interaction energy per residue and the pharmacophore model, allowed us to establish the correlation between biological activity and a set of real numbers called descriptors, to predict the mode of binding of the ligands, the free energies of formation of the different complexes. Molecular docking within the active site of dihydroorotate dehydrogenase showed that the most active inhibitors (Pyl 1 to Pyl 4) exhibit the same binding mode. The RQSA model obtained is closer to experimental reality. Indeed, it explains nearly 97% of the variation in inhibitory activity by the variation in the free enthalpy of formation of the DHODH: Pylx complex.The hydrophobic interactions obtained of Alkyl nature have largely contributed to the stability of the molecules. Subsequently, a residue interaction study made it possible to identify the Val 532 residue as catalytic in the context of DHODH inhibition. The pharmacophore model generated from the poses retained after docking allowed us to identify the regions of the active site which must be occupied by the different hydrophobic groups of the ligand to inhibit the activity of dihydroorotate dehydrogenase.

ABBREVIATIONS

3D: Three-dimensional
CAMD: Computer-aided molecular design
CADTM:Computer-Aided Design of Tailored Molecules
CFF: Consistent Force Field
DHODH:Dihydroorotate dehydrogenase
DS:Discovery Studio
EintMM: enzyme–inhibitor interaction energy
ΔΔGcom : Relative complexation GFE
GFE: Gibbs free energy
HYD: Hydrophobic

HYDA: Hydrophobic Aliphatic
IC_{50}: Inhibitory concentration
IE: Interaction energy
PDB: Protein Data Bank
Pyl: Pyrrole
PH4: Pharmacophore
QSAR: Quantitative structure–activity relationships
RMSD: Root-mean square deviation
SAR: Structure–activity relationships
TS: Training set
VS: Validation set
WHO:World Health Organization

REFERENCES

1. Snow R. W., Guerra C. A., Noor A. M., Myint H. Y., and Hay S. I... The global distribution of clinical episodes of Plasmodium falciparum malaria. *Nature*, 434: pp. 214-217, 2005.

2. Gozalbes R., Mahmoudi N., Mazier D., Danis M., Derouin F.,Nouvellesapproches méthodologiques dans la recherche de molécules antimalariques. *MedTrop*, 64 : pp. 66-70, 2004.

3. Collins, W. E. and Jeffery G. M. "Plasmodium malariae: Parasite and Disease." Clinical Microbiology Reviews 20(4), 579-592, 2007.

4.Golbraikh, A. and A. Tropsha, Predictive QSAR modeling based on diversity sampling of experimental datasets
for the training and test set selection. Journal of Computer-Aided Molecular Design, 16(5/6): p. 357-369, 2002.
5. V.K. Vyas and M. Ghate. Recent Developments in the Medicinal Chemistry and Therapeutic Potential of Dihydroorotate Dehydrogenase (DHODH) Inhibitors. MiniReviews in Medicinal Chemistry, 11: 1039-1055, 2011.

6. Miyazaki Y, Inaoka DK, Shiba T, Saimoto H, Sakura T, Amalia E, Kido Y, Sakai C, Nakamura M, Moore AL, Harada S and Kita K. Selective Cytotoxicity of Dihydroorotate Dehydrogenase Inhibitors to Human Cancer Cells Under Hypoxia and Nutrient-Deprived Conditions. Front. Pharmacol, 9: 997, 2018.

7. I. Fritzson, B. Svensson, S. Al-Karadaghi, B. Walse, U. Wellmar, U.J. Nilsson, D.G. Thrige, and S. Jçnsson. Inhibition of Human DHODH by 4-Hydroxycoumarins, Fenamic Acids, and N-(Alkylcarbonyl) anthranilic Acids Identified by Structure-Guided Fragment Selection. ChemMedChem, 5: 608–617, 2010.

8. Chen R., Weng Z. ZDOCK : An Initial-stage Protein-Docking Algorithm. *Proteins*, 52, 80-87, 2003.

9. Noji, N.; Sunahara, H.; Tsuchiya, K.; Mukai, T.; Komasaka, A.; Ishii, K. Synthesis, 23, 38359-384, 2008.

10. Leroux, F.R.; Manteau, B.; Vors, J-P.; Pazenok, S. Beilstein J. Org. Chem. 4, No. 13, 2008.

11. Jensen F. *Introduction to Computational Chemistry*; John Wiley & Sons, Ltd., 98-149, 2002.

12. Christopher J. Cramer, *Essentials of Computational Chemistry*; John Wiley & Sons, Ltd., 191-232, 2002.

13. Discovery Studio Molecular Modeling and Simulation Program. v2.5. San Diego: Accelrys, Incorp; 2009.

14. Chaquin P. Manual of theoretical chemistry application to structure and reactivity in molecular chemistry. p. 190.

15. Adama Niaré, Hermann N'guessan, Bice Dali, Eugene Megnassan, «Computer-Assisted design of hydroxamic Acid Derivatives inhibitors of M1 Metallo Aminopeptidase of *plasmodium falciparum* with Favorable Pharmacokinetic profile» *British* journal of pharmaceutical Research International, Vol 34, issue 60, P. 21-44, 2022.